INTERNATIONAL SOCIETY FOR SOIL MECHANICS AND GEOTECHNICAL ENGINEERING

SIMSG | ISSMGE

EXPLORING THE EFFECTS OF STRESS HISTORY ON THE DRAINED AND UNDRAINED CYCLIC BEHAVIOUR OF GRANULAR MATERIALS

Daniel BARRETO [1]

ABSTRACT

This paper presents the results of 3D DEM simulations of granular materials subject to cyclic loading. While both the drained and undrained conditions are considered, the effects of depositional history and consolidation stress history on the stress-strain response are specifically evaluated. It is demonstrated that the different stress histories have a significant effect on soil response and that such effects can be attributed to differences in the initial particle arrangement (fabric).

Keywords: cyclic loading, stress history, DEM, undrained, drained

INTRODUCTION

It is widely recognised amongst geotechnical engineers that the laboratory response of granular materials is dependent on the sample preparation method (e.g. Oda, 1972; Miura & Toki, 1982; Vaid & Negussey, 1988). These different methods to prepare samples in the laboratory intend to replicate the mode of particle deposition in the field. The literature available has demonstrated that different deposition methods generate different particle arrangements (fabrics) which account for the subsequent behaviour of soils when subject to external loads.

An ideal technique to analyse the influence of fabric is the Distinct Element Method (DEM). It allows simulating granular materials accounting for their particulate nature. Hence, particle arrangement, inter-particle contact orientations as well as other micro-mechanical quantities can be easily monitored. Furthermore, in contrast to physical experiments, the same numerical sample can be used to model different deposition and stress histories.

Previous DEM research has shown that the macro-scale behaviour of granular materials is the result of an evolving internal micro-structure (fabric) and the transmission of stresses via inter-particle contacts generating complex networks of contact forces. These features can and have been previously quantified (i.e. Thornton, 2000; O'Sullivan et al, 2008). Furthermore, Yimsiri & Soga (2010) have studied the effect of different initial fabrics on the monotonic response of granular assemblies. Note however, that the previous studies have considered either a limited number of cycles when studying cyclic loading, or have compared the undrained and drained response for monotonic loading only.

The present study summarises the results of three-dimensional DEM simulations on numerical specimens when subject to cyclic loading under drained and undrained conditions for 100 cycles, which were sufficient to produce failure in one of the specimens. Two different specimen preparation methods were used in order to obtain different initial fabrics using an approach similar to that proposed by Yimsiri &

---

[1] Lecturer, School of Engineering and the Built Environment, Edinburgh Napier University, e-mail: d.barreto@napier.ac.uk

Soga (2010). In addition, the effect of stress history is examined by considering the response of specimens that were isotropically and anisotropically consolidated. The behaviour of over-consolidated specimens is also assessed.

SIMULATION APPROACH

Three dimensional DEM simulations were performed on polydisperse assemblies containing 4000 spheres and periodic boundary conditions which allow the simulation of element tests free from boundary effects. The grain size distribution was generated using seven different particle sizes with a mean diameter size of 1.1 mm. The DEM algorithm used follows the methodology proposed by Cundall and Strack (1979) and the inter-particle forces are calculated using the Hertz-Mindlin contact model (Mindlin and Deresiewicz, 1953). The properties of the DEM particles are indicated in Table 1. These parameters are commonly used parameters for DEM simulation of glass beads and have been derived experimentally by Cavarreta et al (2010). The simulations are a dynamic process. Particle accelerations are found from the inter-particle forces and calculated using Newton's second law. Integration of the particle accelerations using a finite difference approach provides velocities and updated particle positions. These positions are then used to calculate new inter-particle forces, accelerations, velocities and positions, successively.

Table 1. DEM particle characteristics

PARAMETER	VALUE
Particle density	2.570 kg/m^3
Coefficient of inter-particle friction (μ)	0.235
Poisson's ratio (ν)	0.220
Shear modulus (G)	28.688 GPa

In order to explore the effects of depositional history two different initial fabrics (particle arrangements) were generated. First, starting from a state in which there are no inter-particle contacts, the assembly is compressed to an isotropic stress state of 50 kPa using a servo-controlling algorithm. This generates an assembly with a stable coordination number (average number of inter-particle contacts) and an initial void ratio that is dependent on the coefficient of inter-particle friction (μ) used during the compression stage. In this form, a specimen with an isotropic distribution of inter-particle contacts (i.e. contact orientations are equally distributed in all directions) is generated. On the other hand, an anisotropic fabric was created by pre-straining the isotropic specimen to a large strain value and then re-consolidating it back to the same specified isotropic stress state. Hence, an assembly with contact orientations oriented mainly in the direction of pre-straining (e.g. anisotropic structure) was created. These two initial fabrics are intended to simulate different depositional histories. The initial fabric state of the two specimens was quantified using the methodology proposed by Rothenburgh & Bathurst (1989). In this approach, in order to analyse the contact orientations we consider the vectors normal to the contact. For each contact, a branch vector (**l**) can be constructed connecting the centroids of the two contacting spherical particles, and the unit contact normals can be calculated (**n** = **l**/|**l**|). The fabric can then be described using a probability density function E(**n**) such that
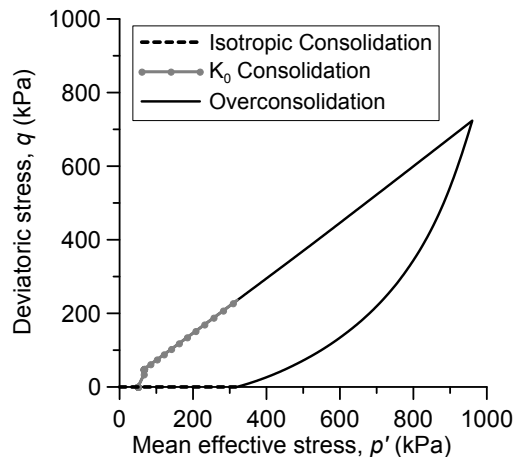
$$\int_{\Omega} E(\boldsymbol{n})d\Omega = 1 \tag{1}$$

where $d\Omega$ is the differential solid angle in a spherical coordinate system. For an assembly that is statistically symmetric about a given axis, (e.g. as in triaxial conditions), the distribution can be represented by a Fourier series (Kanatani, 1984). The Rothenburg and Bathurst equation is given by:

$$E(\theta) = \frac{1}{2\pi}\left\{1 + a\cos 2(\theta - \theta_a)\right\} \qquad (2)$$

where a is a parameter defining the magnitude of fabric anisotropy and θ_a defines the direction of the fabric anisotropy or the principal fabric. Although the direction of fabric anisotropy alternates between 0 and 90° during cyclic loading for triaxial conditions, the magnitude of anisotropy (a) is of particular interest. If the contact orientations are isotropic the value of a is 0.0 and increases as the magnitude of anisotropy increases. a was 0.018 for the isotropic specimen and 0.213 for the anisotropic specimen demonstrating that the initial fabric is very different for both specimens.

In order to study the effects of stress history in addition to the depositional effects described above, different consolidation histories were simulated for both specimens as illustrated in Figure 1. Anisotropically consolidated specimens were generated by vertical compression of the assembly while the radial deformation was kept constant (i.e. $\varepsilon_r = 0\%$ for K_0 conditions) until the same mean effective stress ($p' = (\sigma'_1 + \sigma'_2 + \sigma'_3)/3 = 318$ kPa) as in the isotropically consolidated specimens was reached. Over-consolidated specimens were generated by anisotropic consolidation to a higher deviatoric stress and unloading the specimen under K_0 conditions to the same isotropic stress state of the isotropically consolidated specimens, resulting with an over-consolidation ratio (OCR) of 4.5. The void ratio obtained for the isotropic specimen was 0.528 independently of its consolidation history. Similarly the anisotropic specimen had a void ratio prior to shearing of 0.553. These void ratios correspond to relative densities of 92% and 63%, respectively.

Figure 1. Consolidation stress paths

After consolidation the specimens were cyclically loaded under both drained and 'idealised' undrained conditions starting from a mean effective stress (p') of 318 kPa. Drained shearing was performed by compressing the specimens in the vertical direction while the two horizontal stresses were kept constant. 'Idealised' undrained shearing was performed by maintaining constant volume conditions. Therefore the horizontal deformation in each direction is equal and opposite to half of the vertical deformation. Fluid interaction is not simulated, but since stresses are transmitted (strictly) via inter-particle contacts, the measured stresses in the simulation are effective stresses and the change of pore pressure during undrained loading can be easily calculated. The DEM simulations which will be described in this paper are summarized in Table 2.

Table 2. Summary of simulations

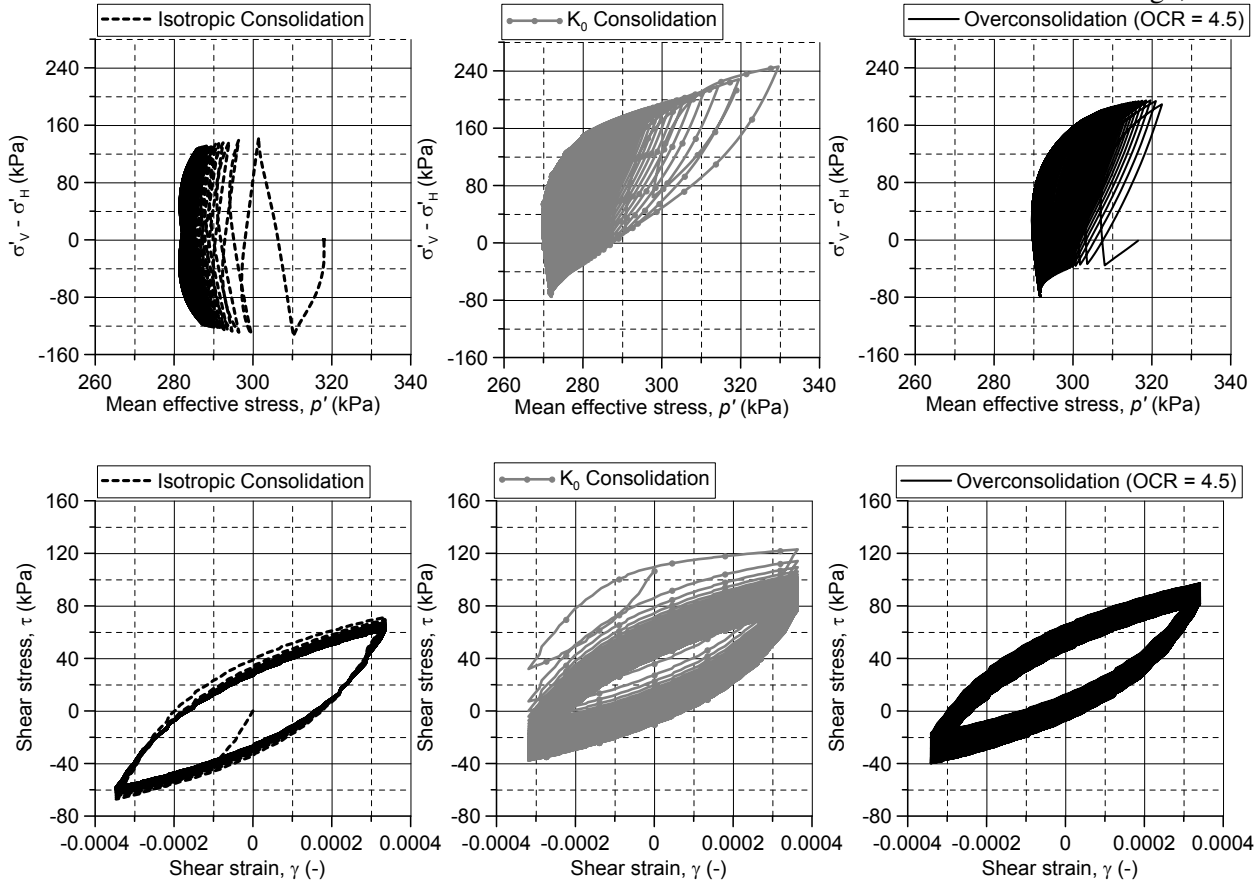| INITIAL FABRIC	CONSOLIDATION TYPE	DRAINAGE	LOADING
Isotropic	Isotropic	Drained	Cyclic
Isotropic	K0	Drained	Cyclic
Isotropic	OCR = 4.5	Drained	Cyclic
Isotropic	Isotropic	Undrained	Cyclic
Isotropic	K0	Undrained	Cyclic
Isotropic	OCR = 4.5	Undrained	Cyclic
Anisotropic	Isotropic	Drained	Cyclic
Anisotropic	Isotropic	Undrained	Cyclic

UNDRAINED CYCLIC LOADING

The effect of consolidation history for cyclic loading under undrained conditions was evaluated by shearing the isotropic specimen ($a = 0.018$) under constant volume conditions after being consolidated following the approach illustrated in Figure 1. The effect of the depositional history (i.e. different initial fabric) was assessed by comparing the behaviour of the isotropically consolidated specimen for both the 'isotropic' and 'anisotropic' initial fabrics.

Effect of consolidation history
Figure 2 shows the undrained stress response of the specimen with initial 'isotropic' fabric when subjected to cyclic loading after the three different consolidation histories simulated as mentioned before. The first column shows the isotropically consolidated specimen; the second column includes the response for the anisotropically consolidated specimen (under K_0 conditions); and the third column presents the over-consolidated specimen (OCR = 4.5). Similarly, the first row illustrates the different stress paths in the triaxial stress space; and the second row draws attention to the cyclic stress-strain response in the τ-γ space. Recall that the three samples evaluated here have the same initial void ratio, sheared under the same level of mean effective stress and with equal cyclic axial strain amplitude ($\varepsilon_a = 0.023\%$). Hence the difference in the response is entirely due to the effect of the consolidation stress path followed prior to shearing. Also note that to facilitate the comparison of results, the scale is the same for all the axes that need to be analysed.

From Figure 2 it can be seen that the anisotropically consolidated sample (second column) differs significantly from the other two. The difference is a direct consequence of the static shear stress at the beginning of shearing which results from the anisotropic consolidation. K_0 consolidation creates a fabric that is more anisotropic than the other two consolidation paths (as quantified by the magnitude of anisotropy, a). This different initial fabric (after consolidation) manifests specially in the first cycles as it can be clearly seen in the stress-strain response. Comparison of the isotropically consolidated specimen and the over-consolidated sample isolates the effect of the static initial shear stress as both specimens are in an isotropic stress state prior to shearing. However, the isotropic stress state for the over-consolidated sample does not correspond to a strictly isotropic fabric. As a consequence, the pore pressure development caused by the deformation of the voids is significantly different and manifests in a very evident manner as observed in the triaxial stress paths.

Figure 3 illustrates additional results in the same way as presented for Figure 2. However, instead of the stress paths and stress-strain response, the pore water pressure changes and the evolution of the shear stress are shown. Once again, the differences for the three different consolidation stress paths are clear.
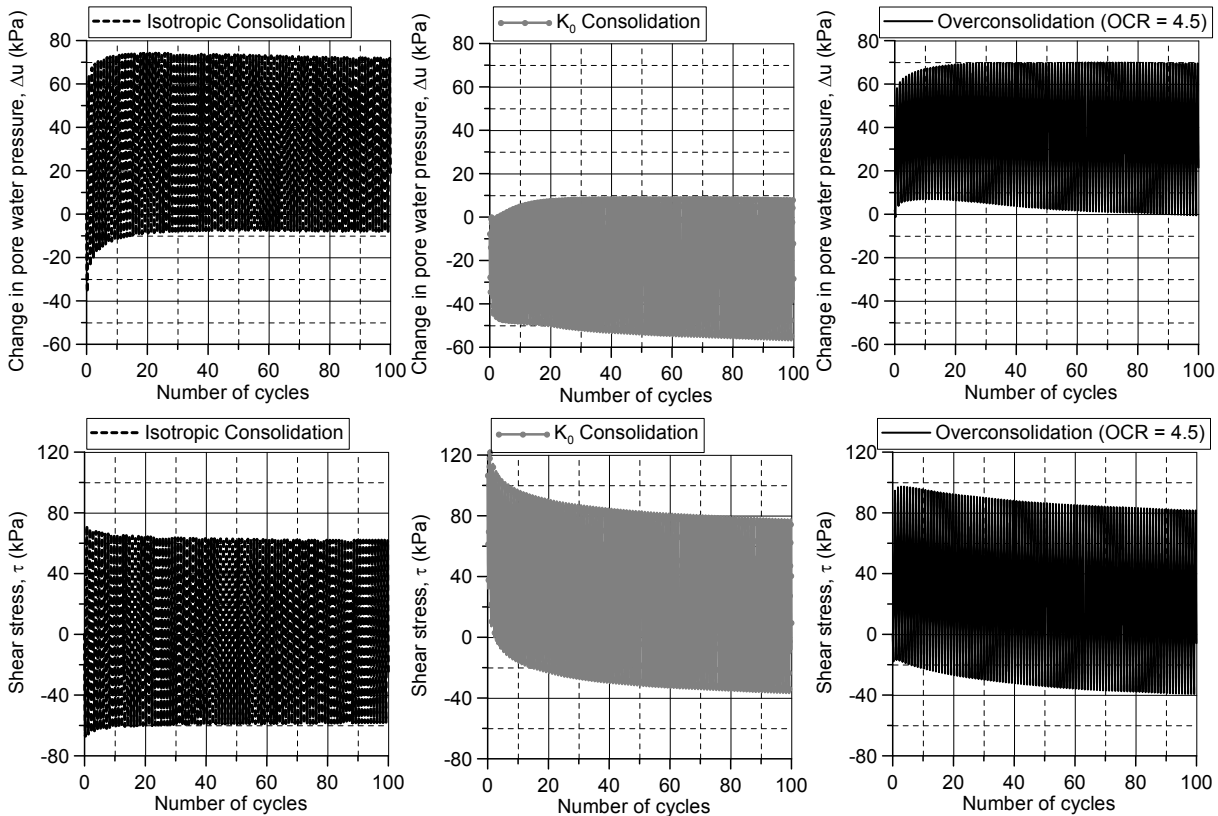
Figure 2. Undrained stress-strain response of a specimen with initial isotropic fabric to different consolidation histories

In relation to the pore water pressure response (i.e. first row in Figure 3), it is interesting to see not only that the amplitude of the change differs for the three specimens, but also that for the over-consolidated specimen there is no negative pore water pressure change as in the other cases. Furthermore, a very different evolution is observed for the three scenarios in the first 10 cycles. The cause of such differences is possibly related to the changes of the void structure, but further research is needed to confirm this statement because the current evidence is not conclusive.
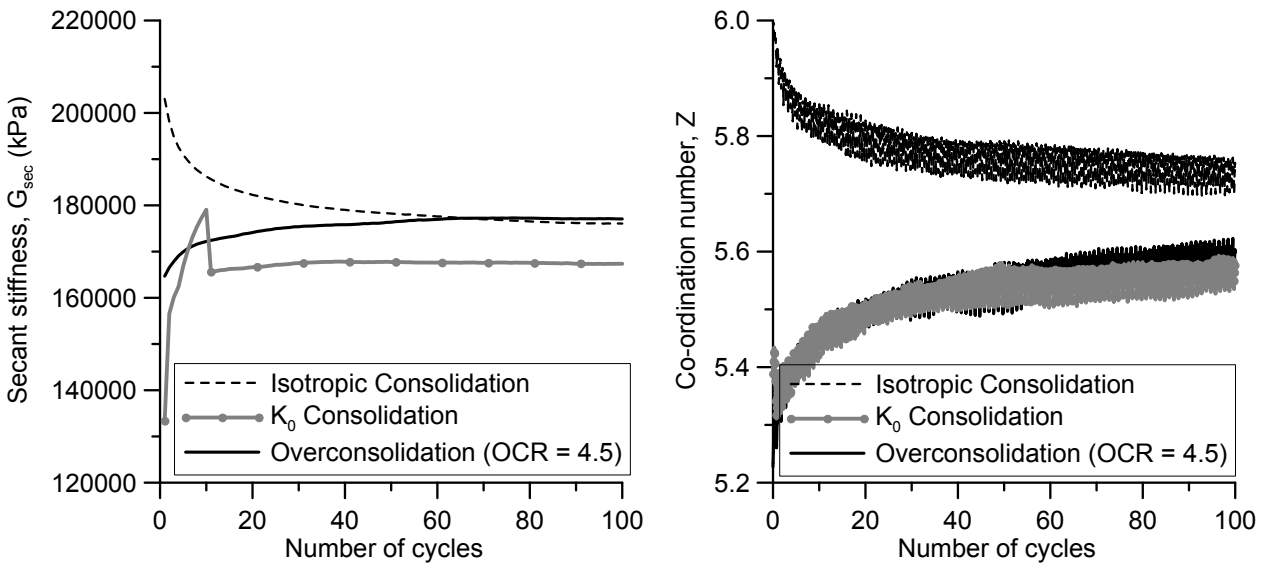
In contrast to pore water pressure regime, from the second row of Figure 3 it can be observed that the amplitude of the shear stress is independent of the consolidation stress history. Also note that the response in the first 10 cycles is different for the three situations under analysis. This result in conjuction with the pore water evolution implies that if the simulations were performed under stress controlled conditions (i.e not strain controlled as presented here), then for a constant cyclic stress amplitude, a different strain amplitude would be developed for the three different consolidation histories. This is in agreement with experimental observations widely available in the existing literature.

From Figure 2 it can be concluded that the stiffness for the three consolidation histories is very similar. The secant stiffness (G_{sec}) defined as the ratio of the difference between the maximum and minimum shear stress over the difference between the maximum and minimum shear strains (i.e. $G_{sec} = (\tau_{max} - \tau_{min})/(\gamma_{max} - \gamma_{min})$) is calculated for the three cases and illustrated in Figure 4a. The stiffnesses are indeed very similar. But it is interesting to observe that while the anisotropically

consolidated and the over-consolidated specimens show a hardening behaviour, the stiffness of the isotropically consolidated specimen degrades as the number of cycles increases.

Figure 3. Evolution of pore water pressure and shear stress for specimen with isotropic initial fabric for different consolidation histories under undrained conditions
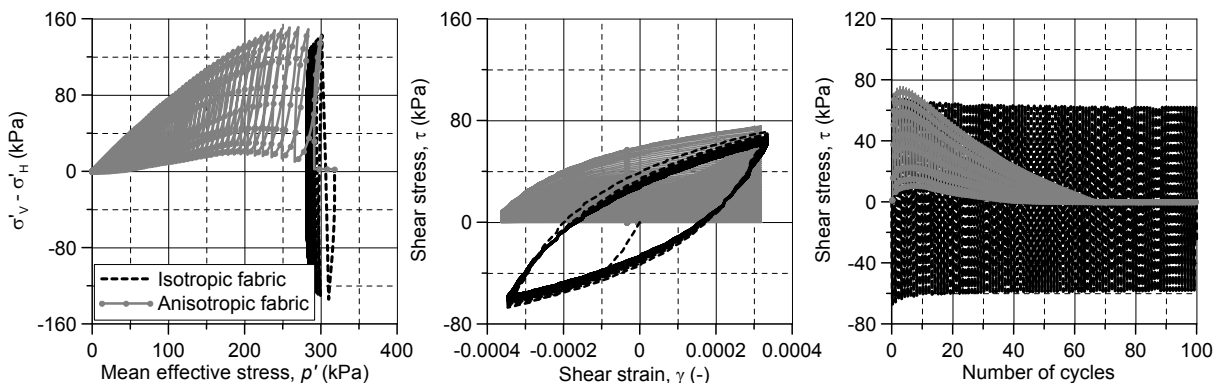

Figure 4. Undrained evolution of secant stiffness and its relationship to the average number of contacts (Z) per particle for specimen with isotropic initial fabric for different consolidation histories

Furthermore, it can be concluded from Figure 4b that such evolution of the stiffness can be explained by the coordination number (equivalent to the average number of contacts per particle). The qualitative behaviour of the coordination number closely resembles that of the evolution of the secant stiffness (G_{sec}). Note that as shearing progresses the coordination number of the isotropically consolidated specimen reduces while it increases for the other two specimens. Whether the three samples converge to a common coordination number at a certain point before or at failure requires further research.

Effect of depositional history

Figure 5 shows the response of two isotropically consolidated samples. The two samples differ in terms of their initial fabric. The sample with anisotropic initial fabric was generated by pre-shearing the specimen with initial isotropic fabric and re-consolidating it back to the same isotropic stress state. It must be said that such a procedure produces samples with completely different initial fabric as mentioned before, but also with different initial void ratios. Whether the observed differences observed in Figure 5 are the result of the different fabric, the different void ratio, or the combination of both is an issue that requires further research. Note however, that the effect of the depositional history (i.e. initial fabric) seems to be significantly higher than the effect of the different stress (consolidation histories) discussed in the previous section.
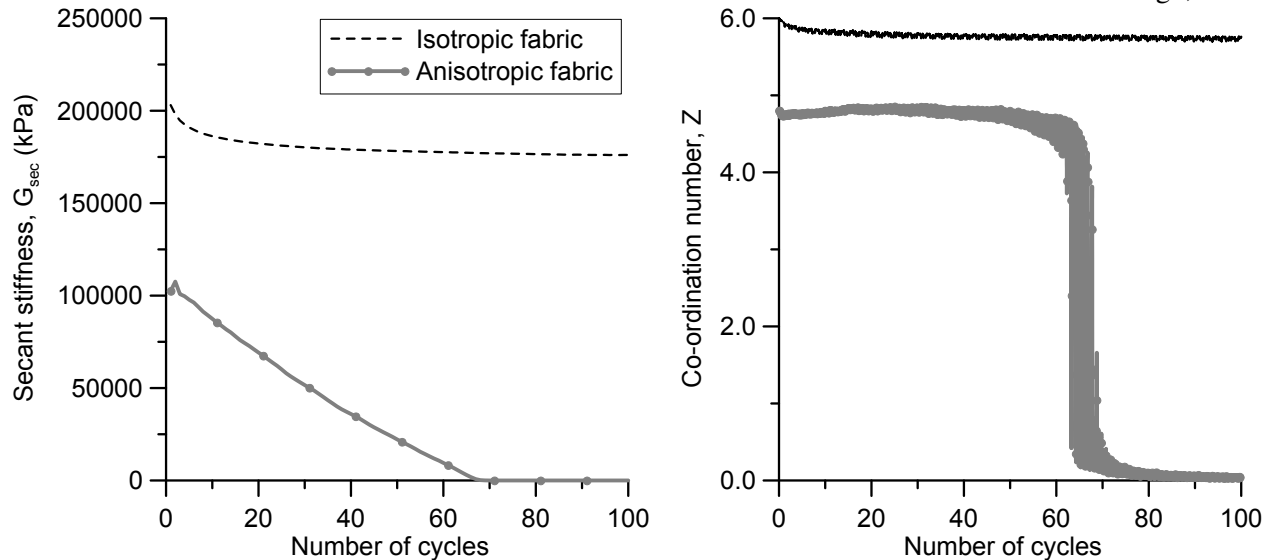

Figure 5. Undrained stress-strain response of specimens with initial isotropic and anisotropic fabric sheared after isotropic consolidation

It can be seen from Figure 5 that the specimen with anisotropic fabric failed after 67 cycles while the isotropic specimen is still very far from such state. The stress-strain response is remarkably different, being considerably softer for the specimen with the initially anisotropic fabric.

Figure 6 highlights the already evident difference in the stiffness behaviour observed in Figure 5b. Note however that the stiffness behaviour is not easily explained in terms of the evolution of the coordination number. Failure is evident in the 67th cycle as observed in Figure 6b. Also note that although there is a sharp reduction in the average number of contacts per particle, this does not correspond with a sharp increase in the pore water pressure. The failure is then characterised in terms of cyclic mobility and not liquefaction.

Although further research is required to confirm such hypothesis, it appears that the results presented above could be explained using a critical state type framework. Since depositional and consolidation history produce different initial fabrics (and densities), it is very likely that such states will be related to a certain distance of the initial state from the critical state line (CSL).

Figure 6. Undrained evolution of secant stiffness and its relationship to the average number of contacts (Z) per particle for specimens with isotropic and anisotropic initial fabric
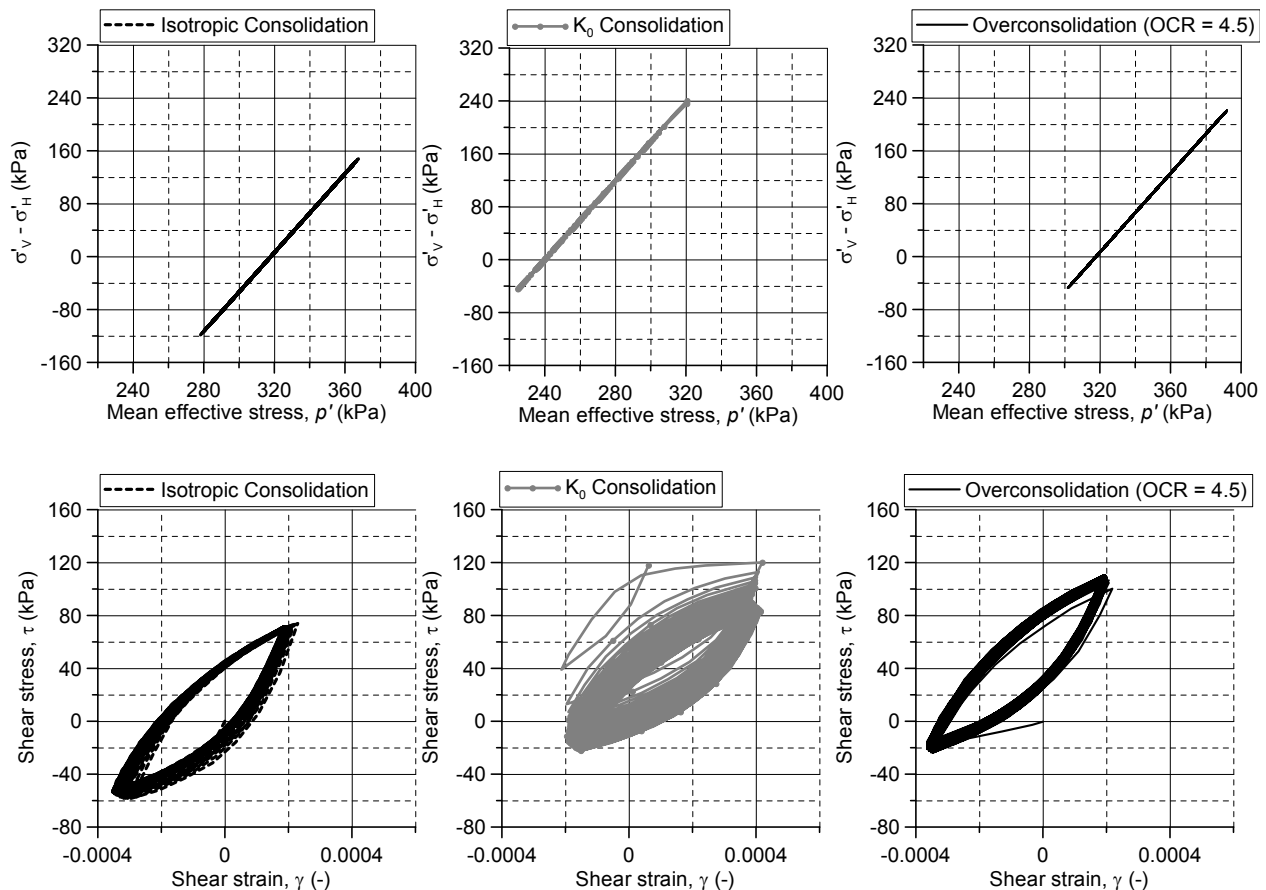
DRAINED CYCLIC LOADING

This section describes the simulation results for the drained conditions. The effects of consolidation history and depositional history are assessed in a manner that is consistent with the discussion regarding the undrained conditions.

Effect of consolidation history

Figure 7 shows the drained stress-strain response for the three different consolidation histories that were analysed under undrained conditions. Their initial void ratio and fabric state is identical to that described for those conditions. The second row shows the stress-strain response in the τ-γ space. The results are very similar to those commented for Figures 2d, e and f and similar observations can be done here. The first row of Figure 7 (a, b and c) shows the typical drained stress path that would be normally expected. Note however that differences exist in the amplitudes of both the mean effective stress and the differences between the vertical and horizontal effective stresses that are developed during cycling. Particularly interesting is the fact that the isotropically consolidated sample experience a much larger extension state in the triaxial stress space even though it starts from the same stress state as the over-consolidated sample. Since the specimens differ only in their initial fabric (e.g. they have equal void ratios, stress states, and cyclic amplitude), the response is a direct consequence of the arrangement of particles that results from the particular consolidation history.

Figure 8 is analogue to Figure 3 but obviously presents the volumetric response instead of the pore water pressure developmet. It can be seen that the results are entirely consistent. Positive pore water pressures in Figure 3 are directly linked to compressive volumetric strains in Figure 8. Similar deductions can be easily made in terms of negative pore pressures and dilative strains. Also note that the comments made regarding the first 10 cycles of shearing during undrained loading can also be made from Figure 8 for the drained conditions.

The development of stiffness for drained conditions deliver similar results to those presented in Figure 4 and are not presented here. Figure 9a shows the evolution of the coordination number and illustrates a striking similarity with Figure 4b (as it should be expected).

Figure 7. Drained stress-strain response of a specimen with initial isotropic fabric to different consolidation histories
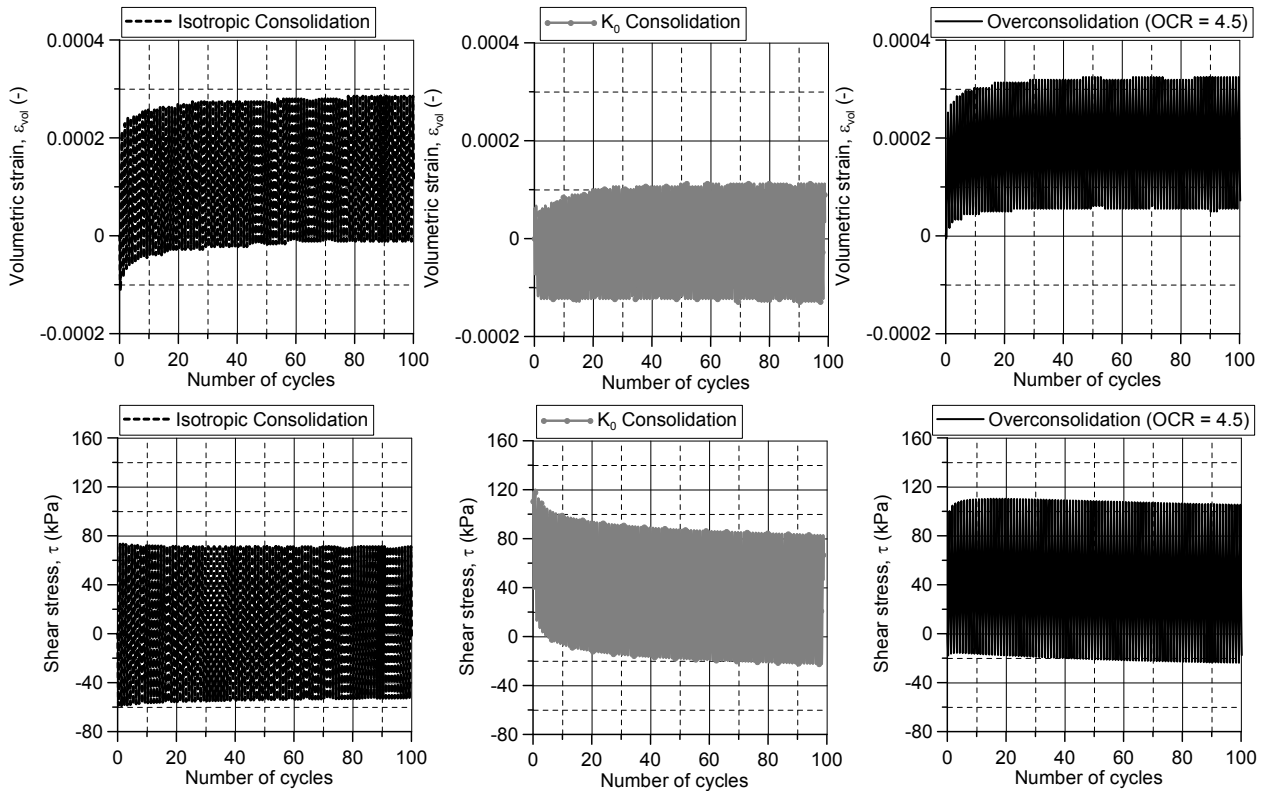
Effect of depositional history

Figure 9b illustrates the evolution of the coordination number for the two specimens that have been isotropically consolidated but that are different in their intial fabric (i.e. depositional history). In contrast to Figure 6b, there is no evident sharp change in the coordination number under drained conditions and failure cannot be identified in such a clear manner as it was done for the undrained conditions. Once again, further research is necessary to consider whether the coordination number will converge to a common value at a larger number of cycles.
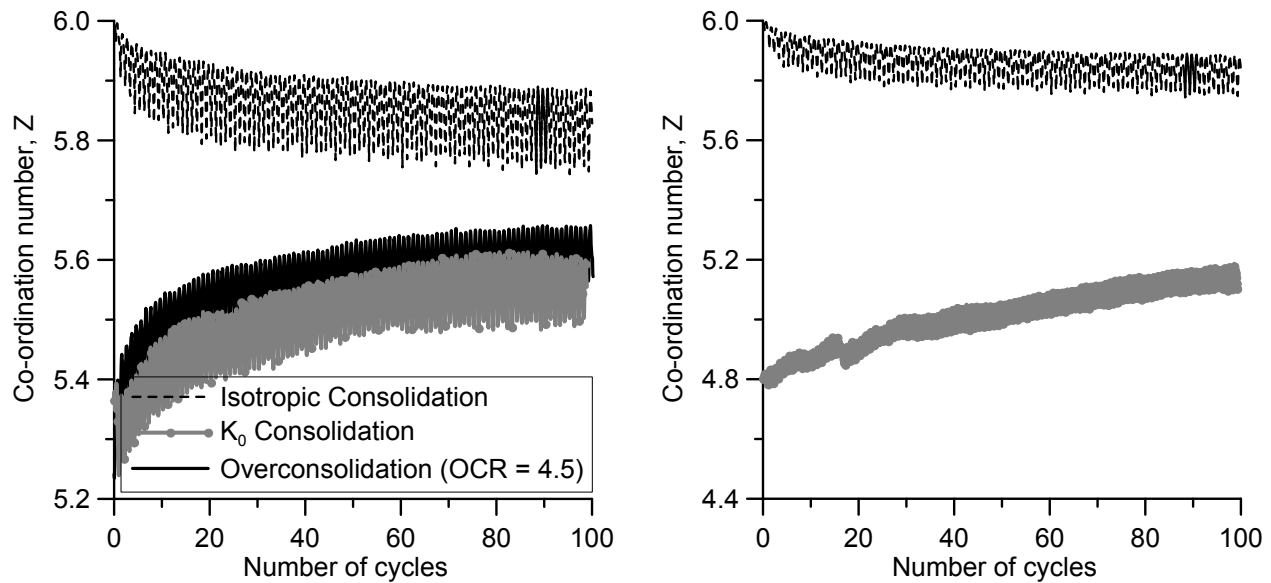
Figure 10 appears to confirm the fact that the effect of depositional history is much more important than the effect produced by the recent consolidation history. From Figure 10b it can be highlighted the similarity with Figure 5a for the undrained case. It is clear that the stress-strain response does not involve stress changes in the extension side of the triaxial stress space. This feature was also observed in the undrained conditons and gives confidence in the results.

The comments regarding the CSL and the relative importance of the initial fabric and the initial density (void ratio) can also be hypothesized here. The results however are not conclusive and comprehensive set of simulations comprising numerous stress states, initial void ratios and magnitudes of anisotropy is required to confirm these results.
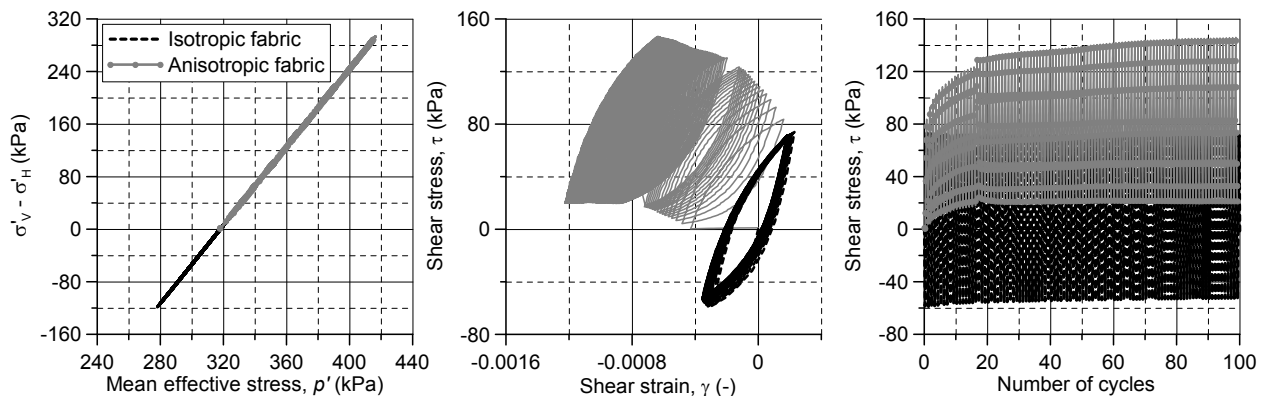
It must also be noted that fabric analyses such as those published by O'Sullivan et al (2008) and Thornton (2000) can provide further insights into the micro-scale interaction underlying the observed macro-scale behaviour. Such analyses will be considered in the future as more data becomes available.

Figure 8. Drained volumetric response and shear stress evolution for specimen with isotropic initial fabric for different consolidation histories

Figure 9. Drained evolution of the average number of contacts (Z) per particle for specimens with isotropic and anisotropic initial fabric in relation to the effect of different consolidation histories

Figure 10. Drained stress-strain response of specimens with initial isotropic and anisotropic fabric sheared after isotropic consolidation

CONCLUSIONS

This study presented the results of 3D DEM simulations on granular assemblies. It considered the effect of depositional and consolidation history under undrained and drained cyclic loading conditions. It was observed that both depositional and consolidation history produce fabric re-arrangement which will subsequently manifest in different stress-strain responses. It seemed clear that the effect of depositional history is significantly higher than that of the consolidation history. Furthermore, it was commented that the differences in behaviour could be explained in terms of micro-mechanical parameters and the relative position of the initial stress state in relation to the critical state line.

REFERENCES

Cavarreta, I., Coop, M. and O'Sullivan, C. (2010), "The influence of particle characteristics on the behaviour of coarse grained soils". Géotechnique, Vol. 60, No. 6, pp. 413–423.

Cundall, P. A. and Strack, O. D. L. (1979), "A discrete numerical model for granular assemblies". Géotechnique, Vol. 29, No. 1, pp. 47–65.

Mindlin, R. D. and Deresiewicz, H. (1953), "Elastic Spheres in Contact under Varying Oblique Forces". Journal of Applied Mechanics, Vol. 20, pp. 327–344.

Kanatani, K. (1984). "Distribution of directional data and fabric tensors", International Journal of Engineering Science, Vol. 22, pp 149 -164.

Miura, K. & Toki, S. (1982). "A sample preparation method and its effect on static and cyclic deformation–strength behaviours of anisotropic sand". Soils and Foundations. Vol. 22. No. 1, pp. 61–77.

Oda, M. (1972). "Initial fabrics and their relations to mechanical properties of granular materials". Soils and Foundations. Vol. 12. No. 1, pp. 16–36.

O'Sullivan, C., Cui, L. & O'Neill, S. C. (2008). " Discrete Element Analysis of the Response of Granular Materials during Cyclic Loading". Vol. 48. No. 4, pp. 511–530.

Rothenburgh, L. & Bathurst, R.J. (1989). "Analytical study of induced anisotropy in idealized granular materials". Géotechnique, Vol. 29, No. 1, pp. 47–65.

Thornton, C. (2000). "Numerical simulations of deviatoric shear deformation of granular media". Géotechnique, Vol. 42, No. 1, pp. 601–614.

Vaid, Y. P. & Negussey, D. (1988). "Preparation of reconstituted sand specimens". ASTM STP 977, pp 405-417

Yimsiri, S. & Soga, K. (2010). "DEM analysis of soil fabric effects on behaviour of sand". Géotechnique, Vol. 60, No. 6, pp. 483–495.